Nanoscale

Accepted Manuscript

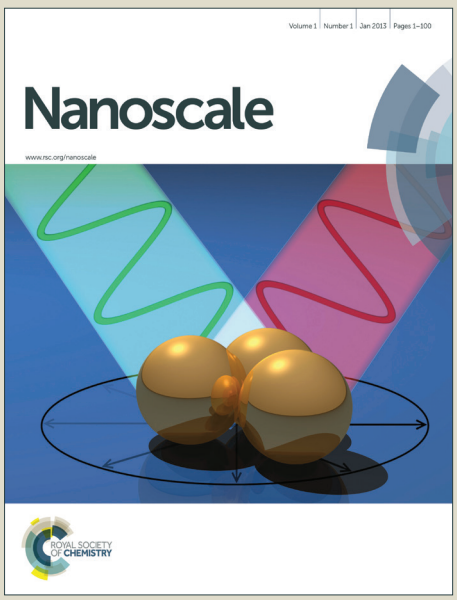

ROYAL SOCIETY OF CHEMISTRY

www.rsc.org/nanoscale

Journal Name

RSCPublishing

ARTICLE

The permeability and transport mechanism of graphene quantum dots (GQDs) across the biological barrier†

Cite this: DOI: 10.1039/x0xx00000x

Received 00th January 2012,
Accepted 00th January 2012

DOI: 10.1039/x0xx00000x

www.rsc.org/

Xin-yi Wang,[a,d] Rong Lei,[b] Hong-duang Huang, [c]Na Wang,[a] Lan Yuan,*[a] Ru-yue Xiao,[a] Li-dan Bai,[a] Xue Li,[a] Li-mei Li[d] and Xiao-da Yang*[a]

As an emerging nanomaterial, graphene quantum dots (GQDs) has showed enormous potential in theranostic applications. However, many aspects of the biological properties of GQDs remain to be clarified. In the present work, we prepared two sizes of GQDs and for the first time investigated their membrane permeability, one of the key factors for all biomedical applications, and transport mechanism on a Madin Darby Canine Kidney (MDCK) cell monolayer. The experimental results revealed that under ~300 mg/L, GQDs were innoxious to MDCK and did not affect the morphology and integrity of the cell monolayer. The P_{app} values were determined to be $1\sim3\times10^{-6}$ cm/s for 12-nm GQDs and $0.5\sim1.5\times10^{-5}$ cm/s for 3-nm GQDs, indicating that the 3-nm GQDs are well-transported species while the 12-nm GQDs have moderate membrane permeable. Transport and uptake of GQDs by MCDK cells were both time and concentration-dependent. Moreover, incubation of cells with GQDs enhanced formation of lipid raft; while inhibition of lipid raft with methyl-β-cyclodextrin almost eliminated membrane transport of GQDs. Overall, the experimental results suggested that GQDs cross the MDCK cell monolayer mainly through a lipid raft-mediated transcytosis. The present work has indicated GQDs as novel low-toxic, high-efficient general carrier for drugs and/or diagnostic agents in biomedical applications.

Introduction

Recently, Graphene quantum dots (GQDs) have attracted much interest in bio-imaging and bio-sensing applications due to their unique intrinsic physical and chemical properties,[1-4] e.g. chemical stability, electronic properties, and photoluminescence. Other than as graphene-based biosensors for detecting biomolecules with high sensitivities, GQDs were also regarded as an ideal candidate for developing novel delivery systems for drugs[5, 6] and genes[7, 8] due to their ultra-high specific surface area and the readily functionalized edge. By combining their diagnostic and therapeutic effects, the multi-functional GQDs will be in the future to become highly competitive for consideration in theranostic applications.[9]

Although GQDs from assorted sources have been prepared and applied to biosensing and bioimaging, and the biosafety and in vivo bio-distribution of GQDs have also been evaluated,[10, 11] to the best of our knowledge, there is limited information on GQD membrane permeability and transport mechanism to support the theranostic application. Previously, the nanotechnology-based drug delivery systems including liposomes,[12] micelles,[13] noble metal nanoparticles,[14] semiconductor materials[15] and metal oxide nanoparticles[16, 17] have been recognized for their ability to pass through the biological barrier and improve drug absorption via two major pathways, transcellular and paracellular pathways.[18] For transcellular pathway, most nanoscale entities crossed the epithelial cell barrier via transcytosis, in which the size[19] and surface properties[20] of nanoparticles were two critical factors. The paracellular pathway was mainly mediated by tight junctions (TJs) and played a key role in regulating or restricting passage of liquids, ions, and larger solutes.[21, 22]The pathway and membrane permeability have been crucial factors determining the fate of any biomaterial as drug carriers and/or diagnostic probes. Therefore, quantitative assessment of GQD membrane permeability and elucidating the mechanism are of great significance for facilitating the biomedical applications of GQDs and biomaterial of similar structures.

In the present work, we prepared two different sizes (3 nm and 12 nm) of GQDs and for the first time evaluated the permeability of GQDs crossing the Madin Darby Canine Kidney (MDCK) cell monolayer, a well-recognized in vitro model for evaluation of drugs and delivery systems across epithelial barriers.[23] Both sizes of GQDs were shown to have low toxicity to MDCK cells and were membrane permeable; while the 3-nm GQDs exhibited much larger apparent permeability coefficient (P_{app}) than the 12-nm GQDs. Nevertheless, both sizes of GQDs were shown to cross the MDCK cell monolayer via a lipid raft-mediated transport process. This transport mechanism indicates the great potential

of small sizes of GQDs as high efficient carrier for drugs and/or diagnostic agents in biomedical applications.

Experimental section

Regents and Materials

MDCK (Madin-Darby canine kidney) cell was obtained from Institute of MateriaMedica, Chinese Academy of Medical Sciences, Beijing. Dulbecco's Modified Eagle's Medium (DMEM), penicillin-streptomycin and fetal bovine serum (FBS) were from GIBCO, Invitrogen Corp. (Carlsbad, CA, USA). Transwells (12 wells, pore diameter of 3 μm, polycarbonate) were supplied from Corning Costar (Cambridge, MA). The MTS tetrazolium compound was from Promega Corp. (Madison, WI, USA). Methyl-β-cyclodextrin (M-β-CD) was purchased from Sigma-Aldrich (St. Louis, MO, USA). All the other reagents were of analytical grade and came from commercial sources.

Graphene Quantum Dots (GQDs) synthesis

A modified method of facile, large scale GQDs synthesis with acidic exfoliation and etching of pitch carbon fibers was conducted as described.[24-26] Briefly, 0.30 g of carbon fibers were pitched into the mixture of concentrated H_2SO_4 (60 mL) and HNO_3 (20 mL). After sufficient sonication, the mixture was stirred for 24 h at desired temperatures (80 °C or 150 °C). After cooling, the solution was diluted with 300 mL of de-ionized water and adjusted to pH 8 with Na_2CO_3. The product solution was purified by dialysis with a retained molecular weight of 1000 Da.

MDCK Cell culture

MDCK cells (under passage 50) were cultured as described[27] in high glucose DMEM supplied with 10% FBS and 1% penicillin-streptomycin, and maintained in a humidified atmosphere containing 5% CO_2 at 37 °C in 25 cm^2 plastic flasks. The medium was refreshed every 2 days. Cells were passaged at 70%-90% confluence using 0.25% (w/v) trypsin-0.02% (w/v) ethylene diaminetetraacetic acid (EDTA) solution.

Cytotoxicity Assay

Toxicity of GQDs was accessed by MTS assay using the CellTiter 96® AQueous One Solution Cell Proliferation Assay kit (Promega Inc., Madison, WI) according to the protocol provided by the manufacturer. Briefly, MDCK cells ($3\sim5\times10^4$ cells/mL) were seeded in 96-well plates (200 μL per well) and left in culture for overnight. Then the cells were incubated with various concentrations of GQDs diluted in DMEM for 2, 6, 12, and 24 h. The cells were then incubated with MTS solution at 37°C for another 1~4 h. Finally, the absorbance at 490 nm was measured on a Thermo Multiskan Ascent plate reader (Thermo Labsystems, Germany).

Lactate Dehydrogenase (LDH) Release Assay

The LDH test-kit (CytoTox-ONE™ Homogeneous Membrane Integrity Assay, Promega Co.) was used to assess the cell membrane integrity. MDCK cells ($3\sim5\times10^3$ cells/well) were seeded in 96-well plates and left in culture for overnight. GQDs samples were then introduced at different concentrations, and the test cultures were incubated for another desired test exposure period (6 and 24 h). No-cell control, untreated cell control and maximum LDH release control were performed on separate plate and assayed. The assays were performed according to the protocol provided by the manufacturer. Fluorescence was measured with an excitation wavelength of 560 nm and an emission wavelength of 590 nm with a FlexStation 3 multifunctional microplate reader (Molecular Devices, USA).

Transport across the MDCK cell monolayer

The MDCK Cells were seeded onto Transwell filters (aperture, 3 μm; diameter, 12 mm) at a density of 1×10^5 cells per well and were allowed to grow and differentiate for 5~7 days.[28] The transepithelial electrical resistance (TEER) of the monolayer was measured with a Millicell electrode resistance system (Millipore). The cell monolayer with net TEER value of >200 $\Omega\cdot cm^2$ were used for transport studies. For the transport experiments, the MDCK cell monolayer was rinsed three times with 37 °C pre-warmed non-fluorescent (NF) DMEM culture media. Samples of GQDs in NF-DMEM were then added to the apical chamber (donor compartment). Samples from the basolateral chamber (receiver compartment) were acquired at desired time intervals to determine the GQD concentrations. The apparent permeability coefficient (P_{app}), was calculated with the following equation:

$$P_{app} = (dQ/dt)/(A\cdot C_0)$$

where dQ/dt was the flux of GQDs across the monolayer (mol transported/sec), A (cm^2, 1.13 cm^2 in the present study) was the surface area of the inserts, and C_0 (M) was the initial GQD concentration in the donor compartment.

Fluorescence spectra of GQDs were obtained on a Hitachi F-7000 fluorescence spectrophotometer (Hitachi, Japan) and absorption spectra were obtained on a Hitachi U-3000 spectrophotometer (Hitachi, Japan). For determination of GQD concentrations, the fluorescence intensity of the samples from receiver compartments was measured with a FlexStation 3 multifunctional microplate reader (Molecular Devices, USA).

To minimize background fluorescence in DMEM media, NF-DMEM were prepared by removal of the fluorescent components including some amino acids (tryptophan, tyrosine, and phenylalanine) and vitamins (folic acid, pyridoxine hydrochloride and riboflavin) from DMEM media. This NF-DMEM maintained the full integrity of the MDCK cell monolayer in the period of transport experiments (data not shown).

To explore the role of lipid raft in GQDs transport, the MDCK cell monolayer was treated with methyl-β-cyclodextrin (M-β-CD) to deplete cholesterol-rich membrane lipid microdomains. Briefly, the MDCK cell monolayer on filters was pre-incubated with 0.5 mM or 5 mM M-β-CD for 30 min at 37oC. After three rinses with NF-DMEM, the transport of GQDs was conducted as described above.

Flow cytometric measurement of cellular uptake

For estimating cellular uptake of GQDs, MDCK cells on 6-well culture plate were incubated with GQDs (28, 140 and 280 mg/L) in DMEM media for 24h. After washing with PBS, the cells were harvested by trypsin digestion. The 1×10^{-6} MDCK cells were then analyzed on a BD Aria SORP flow cytometry (BD Biosciences, San Jose, CA, USA) equipped with a UV laser (355 nm) using FACSDiva version 6.1.0 software (BD Biosciences). GQDs (3 nm) were detected in the FL1 channel

(optical filter at 455/30 nm), and fluorescence of GQDs (12 nm) was detected in the FL3 channel (optical filter at 535/30 nm). For each sample, more than 1×10^4 events were measured.

Immunofluorescence staining of caveolin 1

Lipid raft was visualized by staining the raft proteins with caveolin 1, one of the principal components of caveolae membranes,[29] with the fluorescent antibody previously described.[30, 31] Briefly, MDCK cells on glass bottom cell culture dish were incubated at 37°C with GQDs (20 and 100 mg/L) in DMEM media for 6 h. After treatment, the cells were fixed with 4% paraformaldehyde in PBS and blocked in 2% bovine serum albumin, then incubated with primary antibodies (rabbit polyclonal antibody against caveolin 1) in PBS containing 1% BSA overnight at 4 °C. After rinsing with PBS, cells were incubated with AlexaFluor 488-conjugated secondary antibody and counterstained with Hoechst-33258. The fluorescence was observed on a Leica TCS SP5 laser scanning confocal microscope (Leica Microsystems, Germany). The fluorescence intensity of caveolin 1 was analyzed using an Image-Pro Plus 6.0 software.

Statistics

All the results have been expressed as the mean ± standard deviation (SD). Statistical significance of differences between two groups was determined using student's t-test or one-way analysis of variance (ANOVA). A P-value less than 0.05 were considered statistically significant.

Results and discussion

The size and fluorescent property of GQDs have been controlled by the reaction temperature. Herein, two sizes of GQDs, i.e. ~12 nm and ~3 nm (TEM images of Fig. 1 B and D), were prepared under stirring temperatures of 80°C and 150°C, respectively. At the physiological condition of pH 7.4, the excitation-emission contour plots have been shown in Fig. 1. The 12-nm GQDs (Fig. 1A) exhibited two emission peaks with one at 560 nm upon 460 nm excitation and another at 530 nm with higher quantum efficiency upon 340 nm excitation; while, the 3-nm GQDs (Fig. 1C) exhibited one emission peaks at 430 nm upon two excitation of 265 nm and 330 nm. For fluorescent measurements in the following study, the excitation and emission parameters were: λex/em=340/530 nm for 12-nm GQDs and λex/em=265/430 nm for 3-nm GQDs.

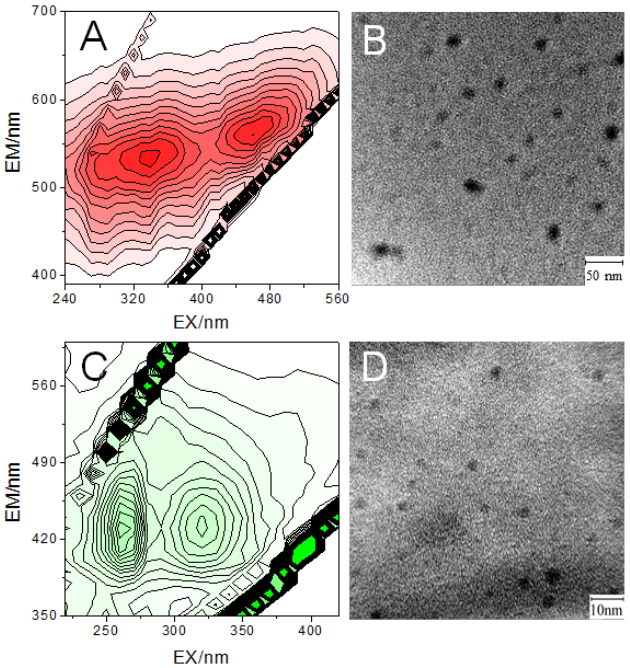

Fig. 1TEM images (B and D) and excitation-emission contour plots (A and C) of GQDs. TEM images showed that the average diameters of GQDs were 12.5±3.6 nm (B) and 3.3±0.7 nm (D), *n*=50.

Consistent with literature reports,[24-26] oxygen-containing groups including carbonyl, carboxyl, hydroxyl, and epoxy groups were introduced to the surface of GQDs as revealed by Fourier transform infrared (FT-IR) spectrum and X-ray photoelectron spectroscopy (XPS) measurements (Fig. S1,ESI†). These oxygen-containing groups revealed that the two sized GQDs as prepared exhibited a hydrophilic and negative-charged surface.

The MTS assays of GQDs on MDCK cells have been shown in Fig. 2. GQDs affected MDCK Cell viability in a both dose- and time-dependent manner. Both were of low toxicity with the larger size GQDs presenting a greater influence on cell viability. Within 6 h at less than 280 mg/L, both GQDs did not significantly reduce cell viability. In another assay for lactate dehydrogenase (LDH) release, 280 mg/L or less of was not observed to cause any damage on plasma membrane (Fig.S3, ESI†). In the MDCK cell monolayer, 280 mg/L GQDs did not alter transepithelial electric resistance (TEER) during the tested time range (6 h). Furthermore, incubation of the MDCK cell monolayer with both sizes of GQDs (280 mg/L) for 24 h did not cause any observable changes in transmission electron microscope (TEM) morphology and ultra-structures of MDCK subcellular organelles (nucleus, villus, mitochondria and endoplasmic reticulum) and tight junction (TJ) between cells(Fig. S2, ESI†).All these results indicated that GQDs do not make holes in the plasma membrane[32] or influence the integrity of cell monolayer, thus causing no problems in the following membrane permeation studies.

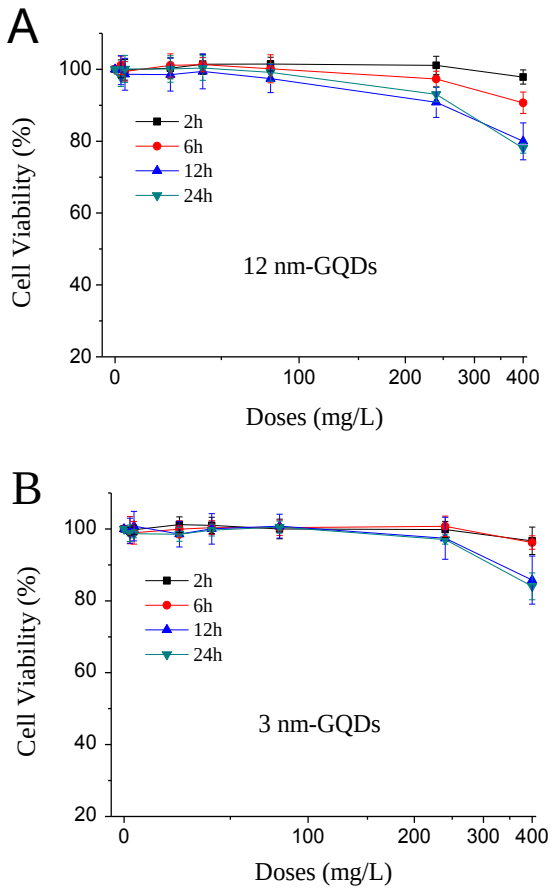

Fig. 2MTS assays of MDCK cells upon treatment with 12-nm GQDs (A) and 3-nm GQDs (B) at 2 h, 6 h, 12 h, and 24 h. Data were the mean ± SD of six replicates.

The membrane permeability is one of the key factors for applications of all biomaterials. To better facilitate theranostic applications, we investigated herein the membrane permeation of GQDs across the MDCK cell monolayer, which has been a well-recognized model for predicting in vivo properties of compounds across the intestinal mucosa and/or blood brain barrier (BBB).It has been suggested that the biological identity of nanoparticles could determine the physiological response including signalling, kinetics, transport, accumulation, and toxicity[33, 34].Considering that GQDs primarily existed in solution as free form by measurement of hydrodynamic sizes in the presence of bovine serum albumin (BSA) (Table S1, ESI†), the present work focused on the intrinsic permeability of GQDs, which would help to predict the transport behaviours in real physiological solutions.

The time courses of membrane permeation of GQDs across the MDCK cell monolayer have been presented in Fig. 3. The amount of transport showed a linear correlation in ~60 min and 180 min for 3-nm and 12-nm GQDs, respectively. Accordingly, the apparent permeability coefficients (P_{app}) for different concentrations of GQDs were for the first time calculated (Fig. 4). Previously, in *vitro* barrier models was suggested to have some defects in assessment of nanoparticle transport due to leak of fluorescent dye labels, nanoparticle agglomeration, and nanoparticles adhering to the basal membrane pores of transwell[35]. However, GQDs herein were assayed by their intrinsic fluorescence and the large GQDs flux (P_{app} of 5~15×10^{-6} cm/s) across the cell monolayer suggest that potential problems caused by nanoparticle agglomeration and nanoparticles adhesion could be neglected.

According to the known P_{app}-bioavailability correlation,[36] 3-nm GQDs (P_{app} of 5~15×10^{-6} cm/s) were the type of a well-transported compounds; while 12-nm GQDs (P_{app} of 1~3×10^{-6} cm/s) were compounds of moderate membrane permeability. This order of permeability is reasonable because larger particles generally have a lower diffusion rate. According to the correlation of diffusion coefficient with the molecular size (D∝ 1/V$^{0.6}$), the ratio of diffusion coefficients for the 3-nm GQDs to 12-nm GQDs was predicted to be 5.2. This theoretical value agreed well with the ratio (4.5~5.4) of P_{app} (Fig. 4) of the two sizes GQDs.

Both P_{app} values increased with concentration of GQDs. This P_{app}-concentration dependency fit well into a Hill model (r^2=0.99998) and the two sizes of GQDs shared a Michaelis constant (K_M) of 131±5 mg/L with the positive cooperative sites (n) of 1.58±0.06. This concentration dependence of P_{app} indicated that transport of GQDs across the MDCK monolayer must be mediated by certain transport vehicles, e.g. membrane channels, carriers, transporters, and/or special lipid phases. Moreover, different sizes of GQDs shared a similar pattern of binding with their transport vehicles.

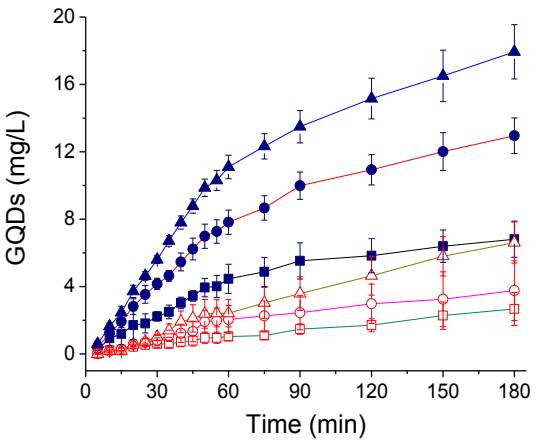

Fig.3 The time course of membrane permeation of GQDs across the MDCK cell monolayer at 70 mg/L (square), 140 mg/L (circle), and 280 mg/L (triangle). Filled symbols for 12-nm GQDs and open symbols for 3-nm GQDs. Data was the mean ± SD of three replicates.

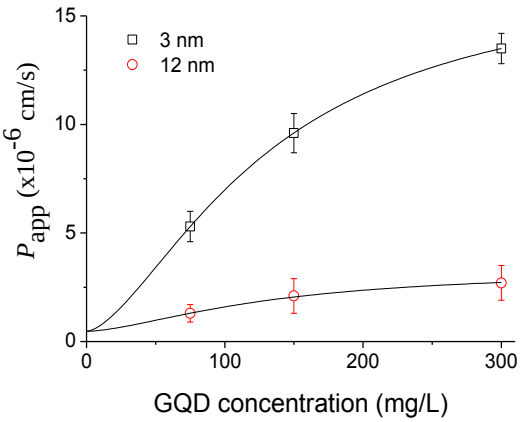

Fig.4The P_{app} of GQDs over different concentrations of GQDs across the MDCK cell monolayer. Open circle symbols for 12-

nm GQDs and open square symbols for 3-nm GQDs. Data was the mean ± SD of three replicates.

Cell uptake is an important evidence for identifying a transcellular pathway across the cell monolayer. Normally, cellular uptake of fluorescent nanoparticles can be visualized with a confocal fluorescence microscope or TEM[37]. Unfortunately, GQDs do not have good visibility and imaging contrast due to not enough electron density or size (Fig.S2, ESI†). In addition, MDCK cells exhibited a high interfering fluorescence background when using the regular excitation filter (355 nm). Therefore, the flow cytometric assay counting a large cell numbers (1×10^4) had to be used for analysis of amounts of endocytosis of GQDs. The fluorescent intensity of the highest 0.1% control cells was set as the gate for estimating the subpopulation of GQDs-content cells (Fig. 5A & C). The results (Fig. 5B & D) showed that GQDs-treatment caused a significant increase of the high-fluorescence subpopulation in a clear dose-dependent manner, indicating the increase of intracellular GQDs uptake with GQDs concentrations.

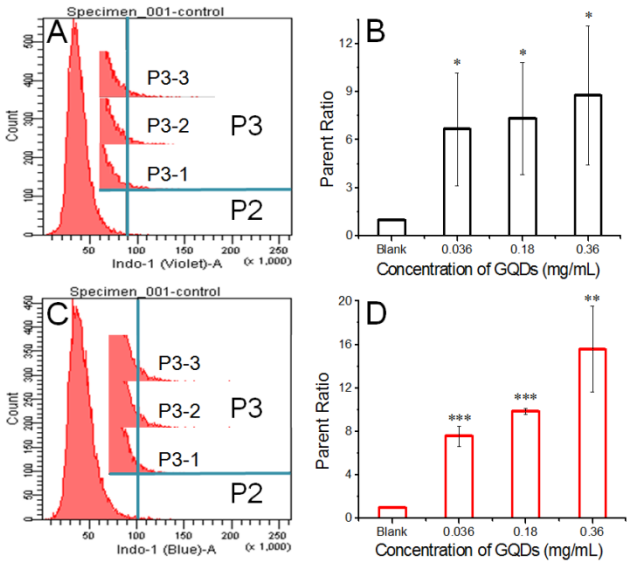

Fig. 5Measurement of GQDs uptake in MDCK cells using fluorescence flow cytometry. A and C were typical flow cytometric histograms for cell uptake of 3-nm and 12-nm GQDs, respectively. Gating strategy to identify GQDs-absorbed cells: P2 for subpopulation of negative control and P3 for subpopulation of GQDs-treated cells (24 h); P3-1, P3-2 and P3-3 for subpopulation of cells treated with 28, 140 and 280 mg/L of GQDs, respectively. B and D were the quantification of cell uptake in A and C, respectively. For each sample, more than 1×10^4 events were measured. Data was the mean ± SD of three replicates. * was for $P< 0.05$, ** was for $P< 0.01$, and *** was for $P< 0.001$ over control.

Considering that lipid raft have been proposed to mediate membrane transport for several nanomaterials,[38, 39] we investigated change of trans-membrane permeation of GQDs in the presence of methyl-β-cyclodextrin (M-β-CD), a classical inhibitor of lipid raft through cholesterol depletion in lipid bilayers.[40, 41] As shown in Fig. 6, pre-treatment of the MDCK cell monolayer bilaterally with M-β-CD for 30 min resulted in significant reduction of P_{app} of both sizes of GQDs in a concentration dependent manner; at 5 mM, M-β-CD almost blocked transport of GQDs. These results indicated a key role of lipid raft in GQDs permeation.

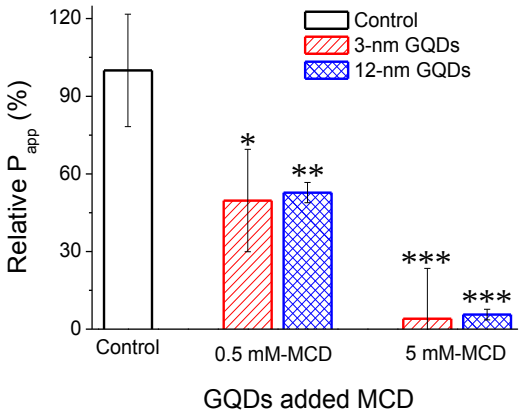

Fig. 6 The effect of M-β-CD treatment on GQDs permeability across the MDCK cell monolayer. Data was the mean ± SD of six replicates. *was for $P < 0.05$, ** was for $P < 0.01$, and *** was for $P < 0.001$ over control.

To investigate the change of lipid raft in the process of GQDs transmembrane permeation, the distribution of a typical raft protein, caveolin 1, was monitored. As shown in Fig. 7, caveolin 1 was present outside the nucleus primarily on plasma membrane as fine fluorescent dots. This is consistent with presence of lipid raft in cell membrane as well as many organelles, e.g. Golgi and lysosomes.[42] Upon incubation with GQDs, the fluorescence intensity of caveolin 1 increased in a dose-dependent manner and the protein appeared to aggregate into larger spots. Both sizes GQDs exhibited a similar effect on caveolin 1 distribution. This indicated that lipid raft may interact with GQDs on both the cell plasma membrane and the cytoplasmic compartment, thus suggesting that lipid raft may participate in the process of GQDs intracellular trafficking.

Binding of a substrate to its vehicle is the initial step for membrane transport. As the structure of GQDs is featured by a bulk single graphene sheet and more reactive edges, GQDs could react with non-polar molecules through weak hydrophobic interactions or with electron-defect compounds (e.g. metal ions[43] and positive-charge organic agents[44]) through strong electron-transfer interaction. The K_M value corresponded to a relatively small free energy change of $\Delta G = -RT\ln(1/K_M) =$ -15.6 kJ/mol per six-carbon-ring unit, this binding energy falls into the range of hydrophobic interaction (10-20 kJ per mole of hydrophobic group). Thus, a hydrophobic interaction between GQDs and lipid raft is suggested.

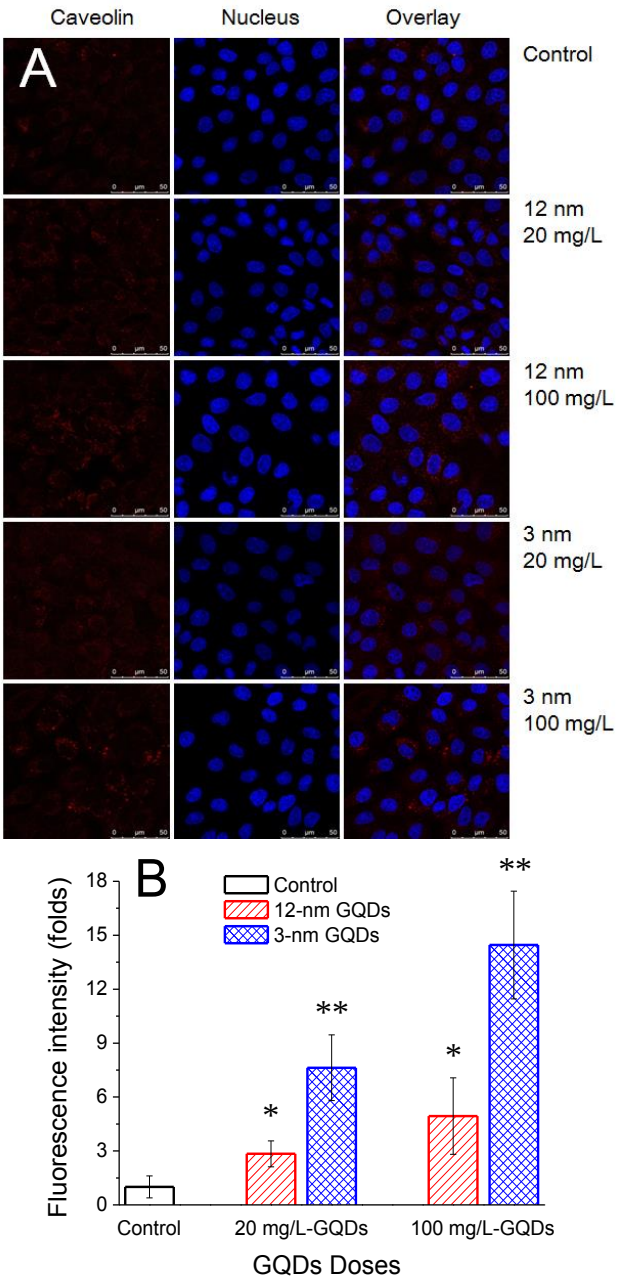

Fig. 7 Fluorescence image of lipid raft visualized by the lipid raft protein, caveolin 1. A: typical immunofluorescence images with rabbit polyclonal antibody against caveolin 1 antibody; B: quantification of vaveolin-1 fluorescence in A. Data was the mean ± SD of three replicates. * was for $P < 0.05$, ** was for $P < 0.01$, and *** was for $P < 0.001$ over control.

Based on the above observation and discussion, we proposed a putative mechanism for the membrane transport of GQDs (Scheme 1): First, when incubated with cells, GQDs bind to lipid raft through hydrophobic interaction. Next, GQDs assembled into the lipid bilayer probably in a similar manner to that of raft proteins as high density nanoclusters. Since the size of raft proteins ranged over 5-20 nm, GQDs of sizes less than 5 nm would be preferable. However, GQDs assembly into lipid raft may compromise the fluorescence of GQDs and thus GQDs modification may be necessary to retain the luminescence properties inside cells when used as fluorescent probes. Next, GQDs associated with lipid raft would move in and out the cytosol through endocytosis or exocytosis and were also distributed inside cytosol.

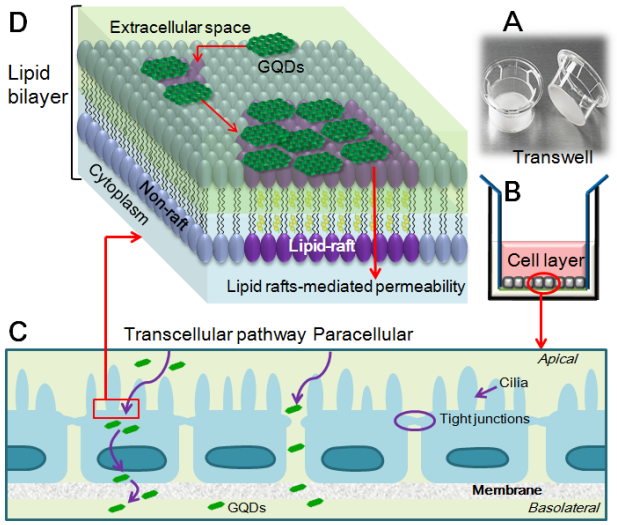

Scheme1 Illustration of the putative mechanism for membrane of GQDs across the MDCK cell monolayer. A: the photo of Transwell insert; B: the schematics of the experimental design; C: the process of GQDs transport across the MDCK cell monolayer; D: lipid raft-mediated transcytosis of GQDs.

Conclusions

The present work investigated the transport properties of GQDs across the MDCK cell monolayer. The experimental results revealed that GQDs crossed cell membrane with good permeability through a lipid raft-mediated transcytosis; thus, the smaller size GQDs exhibited higher membrane permeability. The present work supported GQDs as a novel low-toxic but high-efficient general carrier for drug and/or diagnostic agents in biomedical applications.

Acknowledgements

This work was supported by National Natural Science Foundation of China (No. 21271012), Founder Research Fund for Drug Discovery and Innovation, and Education Department of Liaoning Province (No. L2011108).

Notes and references

[a] State Key laboratories of Natural and mimetic drugs and Department of Chemical Biology, School of Pharmaceutical Sciences, Peking University, Beijing 100083, China. Fax: +86-10-62015584; Tel: +86-10-82801539; E-mail: xyang@bjmu.edu.cn.

[b] Institute of Plant Quarantine of China, Chinese Academy of Inspection and Quarantine, Beijing 100029, China.

[c] College of Chemistry and Molecular Engineering, Peking University, Beijing 100871, China.

[d] College of Sciences, Shenyang Agricultural University, Shenyang 110161, China.

†Electronic Supplementary Information (ESI) available: Fig.S1-S2. See DOI: 10.1039/c000000x/

1. S. J. Zhu, J. H. Zhang, C. Y. Qiao, S. J. Tang, Y. F. Li, W. J. Yuan, B. Li, L. Tian, F. Liu, R. Hu, H. N. Gao, H. T. Wei, H. Zhang, H. C. Sun and B. Yang, *Chem. Commun.*, 2011, **47**, 6858-6860.
2. S. J. Zhu, J. H. Zhang, S. J. Tang, C. Y. Qiao, L. Wang, H. Y. Wang, X. Liu, B. Li, Y. F. Li, W. L. Yu, X. F. Wang, H. C. Sun and B. Yang, *Adv. Funct. Mater.*, 2012, **22**, 4732-4740.
3. L. L. Li, G. H. Wu, G. H. Yang, J. Peng, J. W. Zhao and J. J. Zhu, *Nanoscale*, 2013, **5**, 4015-4039.
4. W. L. Wei and X. G. Qu, *Small*, 2012, **8**, 2138-2151.
5. Z. Liu, J. T. Robinson, X. M. Sun and H. J. Dai, *J. Am. Chem. Soc.*, 2008, **130**, 10876-+.
6. B. Tian, C. Wang, S. Zhang, L. Z. Feng and Z. Liu, *Acs Nano*, 2011, **5**, 7000-7009.
7. H. Dong, L. Ding, F. Yan, H. Ji and H. Ju, *Biomaterials*, 2011, **32**, 3875-3882.
8. X. Y. Yang, G. L. Niu, X. F. Cao, Y. K. Wen, R. Xiang, H. Q. Duan and Y. S. Chen, *J. Mater. Chem.*, 2012, **22**, 6649-6654.
9. K. Yang, L. Z. Feng, X. Z. Shi and Z. Liu, *Chem. Soc. Rev.*, 2013, **42**, 530-547.
10. M. Nurunnabi, Z. Khatun, K. M. Huh, S. Y. Park, D. Y. Lee, K. J. Cho and Y. K. Lee, *Acs Nano*, 2013, **7**, 6858-6867.
11. K. Yang, Y. J. Li, X. F. Tan, R. Peng and Z. Liu, *Small*, 2013, **9**, 1492-1503.
12. G. Cevc, *Adv. Drug Del. Rev.*, 2004, **56**, 675-711.
13. Y. Miura, T. Takenaka, K. Toh, S. R. Wu, H. Nishihara, M. R. Kano, Y. Ino, T. Nomoto, Y. Matsumoto, H. Koyama, H. Cabral, N. Nishiyama and K. Kataoka, *Acs Nano*, 2013, **7**, 8583-8592.
14. G. F. Paciotti, D. G. I. Kingston and L. Tamarkin, *Drug Dev. Res.*, 2006, **67**, 47-54.
15. K. T. Yong, Y. C. Wang, I. Roy, H. Rui, M. T. Swihart, W. C. Law, S. K. Kwak, L. Ye, J. W. Liu, S. D. Mahajan and J. L. Reynolds, *Theranostics*, 2012, **2**, 681-694.
16. O. Veiseh, J. W. Gunn and M. Q. Zhang, *Adv. Drug Deliv. Rev.*, 2010, **62**, 284-304.
17. H. L. Liu, M. Y. Hua, H. W. Yang, C. Y. Huang, P. C. Chu, J. S. Wu, I. C. Tseng, J. J. Wang, T. C. Yen, P. Y. Chen and K. C. Wei, *Proc. Natl. Acad. Sci. U. S. A.*, 2010, **107**, 15205-15210.
18. I. C. Lin, M. T. Liang, T. Y. Liu, Z. M. Ziora, M. J. Monteiro and I. Toth, *Biomacromolecules*, 2011, **12**, 1339-1348.
19. I. Canton and G. Battaglia, *Chem. Soc. Rev.*, 2012, **41**, 2718-2739.
20. J. Nam, N. Won, J. Bang, H. Jin, J. Park, S. Jung, S. Jung, Y. Park and S. Kim, *Adv. Drug Deliv. Rev.*, 2013, **65**, 622-648.
21. P. Artursson and R. T. Borchardt, *Pharm. Res.*, 1997, **14**, 1655-1658.
22. C. R. Weber, in *Barriers and Channels Formed by Tight Junction Proteins I*, eds. M. Fromm and J. D. Schulzke, Blackwell Science Publ, Oxford, 2012, vol. 1257, pp. 77-84.
23. D. A. Volpe, *Future Med. Chem.*, 2011, **3**, 2063-2077.
24. M. Nurunnabi, Z. Khatun, G. R. Reeck, D. Y. Lee and Y. K. Lee, *Chem. Commun.*, 2013, **49**, 5079-5081.
25. M. M. Xie, Y. J. Su, X. N. Lu, Y. Z. Zhang, Z. Yang and Y. F. Zhang, *Mater. Lett.*, 2013, **93**, 161-164.
26. J. Peng, W. Gao, B. K. Gupta, Z. Liu, R. Romero-Aburto, L. H. Ge, L. Song, L. B. Alemany, X. B. Zhan, G. H. Gao, S. A. Vithayathil, B. A. Kaipparettu, A. A. Marti, T. Hayashi, J. J. Zhu and P. M. Ajayan, *Nano Lett.*, 2012, **12**, 844-849.
27. Y. Zhang, X. D. Yang and K. Wang, *Chin. Sci. Bull.*, 2005, **50**, 1854-1859.
28. Y. Zhang, X. D. Yang, K. Wang and D. C. Crans, *J. Inorg. Biochem.*, 2006, **100**, 80-87.
29. C. M. Thomas and E. J. Smart, *J. Cell. Mol. Med.*, 2008, **12**, 796-809.
30. W. S. Bush, G. Ihrke, J. M. Robinson and A. K. Kenworthy, *Histochem. Cell Biol.*, 2006, **126**, 27-34.
31. W. K. Lo, C. J. Zhou and J. Reddan, *Exp. Eye Res.*, 2004, **79**, 487-498.
32. E. Frohlich, *International Journal of Nanomedicine*, 2012, **7**, 5577-5591.
33. C. D. Walkey and W. C. W. Chan, *Chem. Soc. Rev.*, 2012, **41**, 2780-2799.
34. M. P. Monopoli, D. Walczyk, A. Campbell, G. Elia, I. Lynch, F. B. Bombelli and K. A. Dawson, *J. Am. Chem. Soc.*, 2011, **133**, 2525-2534.
35. D. Ye, M. N. Raghnaill, M. Bramini, E. Mahon, C. Aberg, A. Salvati and K. A. Dawson, *Nanoscale*, 2013, **5**, 11153-11165.
36. P. Artursson, *J. Pharm. Sci.*, 1990, **79**, 476-482.
37. D. Ye, K. A. Dawson and I. Lynch, *Analyst*, 2015.
38. R. G. Parton and A. A. Richards, *Traffic*, 2003, **4**, 724-738.
39. B. He, Z. R. Jia, W. W. Du, C. Yu, Y. C. Fan, W. B. Dai, L. Yuan, H. Zhang, X. Q. Wang, J. C. Wang, X. Zhang and Q. Zhang, *Biomaterials*, 2013, **34**, 4309-4326.
40. A. E. Christian, M. P. Haynes, M. C. Phillips and G. H. Rothblat, *J. Lipid Res.*, 1997, **38**, 2264-2272.
41. R. Zidovetzki and I. Levitan, *Biochim. Biophys. Acta*, 2007, **1768**, 1311-1324.
42. D. Lingwood and K. Simons, *Science*, 2010, **327**, 46-50.
43. H. D. Huang, L. Liao, X. Xu, M. J. Zou, F. Liu and N. Li, *Talanta*, 2013, **117**, 152-157.
44. R. Sharma, J. H. Baik, C. J. Perera and M. S. Strano, *Nano Lett.*, 2010, **10**, 398-405.